Reduction of All-*trans* Retinal to All-*trans* Retinol in the Outer Segments of Frog and Mouse Rod Photoreceptors

Chunhe Chen,* Efthymia Tsina,† M. Carter Cornwall,† Rosalie K. Crouch,‡ Sukumar Vijayaraghavan,* and Yiannis Koutalos‡

*Department of Physiology and Biophysics, University of Colorado School of Medicine, Denver, Colorado;
†Department of Physiology and Biophysics, Boston University School of Medicine, Boston, Massachusetts; and
‡Department of Ophthalmology, Medical University of South Carolina, Charleston, South Carolina

ABSTRACT The first step in the Visual Cycle, the series of reactions that regenerate the vertebrate visual pigment rhodopsin, is the reduction of all-*trans* retinal to all-*trans* retinol, a reaction that requires NADPH. We have used the fluorescence of all-*trans* retinol to study this reduction in living rod photoreceptors. After the bleaching of rhodopsin, fluorescence (excitation, 360 nm; emission, 457 or 540 nm) appears in frog and wild-type mouse rod outer segments reaching a maximum in 30–60 min at room temperature. With this excitation and emission, the mitochondrial-rich ellipsoid region of the cells shows strong fluorescence as well. Fluorescence measurements at different emission wavelengths establish that the outer segment and ellipsoid signals originate from all-*trans* retinol and reduced pyridine nucleotides, respectively. Using outer segment fluorescence as a measure of all-*trans* retinol formation, we find that in frog rod photoreceptors the NADPH necessary for the reduction of all-*trans* retinal can be supplied by both cytoplasmic and mitochondrial metabolic pathways. Inhibition of the reduction reaction, either by retinoic acid or through suppression of metabolic activity, reduced the formation of retinol. Finally, there are no significant fluorescence changes after bleaching in the rod outer segments of *Rpe*65$^{-/-}$ mice, which lack 11-*cis* retinal.

INTRODUCTION

The first step of the visual transduction process in vertebrate photoreceptors is the photoisomerization of the visual pigment chromophore from its 11-*cis* conformation to all-*trans*. The isomerization leads to the formation of photoactivated rhodopsin, which begins the cascade of reactions constituting visual phototransduction (for reviews see Ebrey and Koutalos, 2001; Fain et al., 2001). Photoactivated rhodopsin is deactivated through phosphorylation by rhodopsin kinase and capping by arrestin. Subsequently, all-*trans* retinal dissociates from the protein and is recycled to form 11-*cis* retinal through a series of reactions called the Visual Cycle. The first step in this cycle occurs in the photoreceptor outer segment. All-*trans* retinal is reduced to all-*trans* retinol by the photoreceptor retinol dehydrogenase, in a reaction utilizing NADPH (Futterman et al., 1970; Palczewski et al., 1994). Then, retinol is removed from the outer segment presumably by lipophilic carriers present in the interphotoreceptor matrix, such as serum albumin and interphotoreceptor matrix retinoid binding protein (IRBP) (Adler and Edwards, 2000). The retinol is transferred to the retinal pigment epithelium (RPE) (Okajima et al., 1990), where it is converted to retinyl ester (Saari et al., 1993). The ester is isomerized to form 11-*cis* retinol (Bernstein and Rando, 1986; McBee et al., 2000), which is oxidized to 11-*cis* retinal. 11-*cis* Retinal is transported back to photoreceptor outer segments to regenerate rhodopsin. The regeneration of the pigment takes a long time for rod photoreceptors, which are responsible for vision at low light intensities. On the other hand, cone photoreceptors, which are responsible for vision at high light intensities, regenerate their pigment much faster, perhaps through the use of another pathway that involves the retinal Müller cells (Mata et al., 2002).

We have followed the approach of Tsina et al. (2004) and taken advantage of the intrinsic fluorescence of all-*trans* retinol to study its formation in the outer segments of living rod photoreceptors from frog and mouse. Frog rod photoreceptors are large, robust, contain a single chromophore, and can survive isolated for several hours, allowing extensive experimental manipulations. Mouse rod photoreceptors are much smaller and fragile, but allow the use of genetically modified animals. We demonstrate that the fluorescence appearing in rod outer segments after bleaching of rhodopsin is distinct from the fluorescence of the rich in mitochondria ellipsoid region of the cells; we establish that the outer segment fluorescence signal is due to retinol, whereas that of the ellipsoid region is due to NAD(P)H . We have probed the metabolic requirements for the formation of all-*trans* retinol after rhodopsin bleaching and find that the required NADPH can be produced through several metabolic pathways. We also find that inhibition of the reduction step, either by retinoic acid, a retinol dehydrogenase inhibitor, or through suppression of metabolic activity, reduces the level of retinol reached in the outer segment, in agreement with the step being kinetically important as previously proposed. However, this inhibition does not increase the time it takes for the retinol concentration to reach a steady state, as it would have been expected if the reduction were the only slow step. As

Submitted October 8, 2004, and accepted for publication December 17, 2004.

Address reprint requests to Dr. Yiannis Koutalos, Dept. of Ophthalmology, Medical University of South Carolina, 167 Ashley Ave., Charleston, SC 29425. Tel.: 843-792-9180; Fax: 843-792-4096; E-mail: koutalo@musc.edu.

© 2005 by the Biophysical Society

0006-3495/05/03/2278/10 $2.00

doi: 10.1529/biophysj.104.054254

expected, we do not observe any significant fluorescence changes after bleaching in the rod outer segments of *Rpe*65$^{-/-}$ mice, which lack 11-*cis* retinal.

MATERIALS AND METHODS

Grass frogs (*Rana pipiens*; Blue Spruce Biological Supply, Castle Rock, CO) were used to obtain living, isolated rod photoreceptor cells. Procedures for obtaining isolated photoreceptor cells have been described in detail elsewhere (Koutalos et al., 1995; Nakatani et al., 2002). Briefly, an animal was dark-adapted for 2–3 hr, sacrificed, and the retinas excised in the dark with the help of infrared image converters. Isolated photoreceptor cells were obtained by chopping the retina with a razor blade under Ringer's solution in a petri dish coated with Sylgard elastomer. The composition of the amphibian Ringer's solution in mM is: 110 NaCl, 2.5 KCl, 1.6 $MgCl_2$, 1 $CaCl_2$, 5 HEPES, 5 glucose, pH = 7.55. Isolated cells in Ringer's were transferred to 100-μL chambers that fit on the microscope stage. This procedure results mostly in rod photoreceptor cells that have broken below the ellipsoid region, although intact cells are obtained as well. Rod outer segments with attached ellipsoid (ROS-RIS preparation) are viable and metabolically competent (Biernbaum and Bownds, 1985).

We have inhibited different metabolic pathways as follows: a), to inhibit glycolysis and the pentose phospate pathway, we employed 10 mM deoxyglucose, an inhibitor of glucose phosphorylation (Kletzien and Perdue, 1973), in the absence of glucose; b), to deplete mitochondrial NAD(P)H pools and also stop mitochondrial generation of ATP, we employed 10 μM FCCP (an uncoupler of oxidative phosphorylation) and 5 μM oligomycin (an inhibitor of the mitochondrial ATP-synthase; Hoppe et al., 1986); and c), to inhibit the supply of mitochondrial metabolites like isocitrate to cytosolic $NADP^+$-dependent dehydrogenases, we employed 1 mM 1,2,3-benzenetricarboxylic acid (1,2,3-BTC; a specific inhibitor of the mitochondrial tricarboxylate transporter; Parlo and Coleman, 1986). These inhibitory treatments were used separately and in different combinations. Deoxyglucose, 1,2,3-BTC and 1,2,4-BTC were dissolved directly into buffer, whereas FCCP and oligomycin were diluted from stock solutions in dimethylsulfoxide (DMSO). The final DMSO concentration was no more than 0.1%, which in control experiments was shown to have no effect.

Experiments on mouse rod photoreceptors were carried out with slices of retinas from wild-type (strains C57BL/6, SV129, CD1, FVB) mice and genetically modified (knockout) mice lacking the *Rpe*65 protein (*Rpe*65$^{-/-}$). The *Rpe*65$^{-/-}$ animals (Redmond et al., 1998) were kindly provided by Dr. M. Redmond at the National Eye Institute. The animals were male or female. For wild-type, the animal ages used were typically 2–6 months old, whereas for the *Rpe*65$^{-/-}$ were 2–3 months old. We did not detect any dependence of the results on the strain, sex, or age of the animals. Animals were dark-adapted overnight, sacrificed in dim red light and the eyes were enucleated; subsequently the retinas were excised under infrared illumination and placed in mammalian Ringer's slightly modified from He et al. (2000) and Winkler (1981) with a composition in mM: 130 NaCl, 5 KCl, 0.5 $MgCl_2$, 2 $CaCl_2$, 25 HEPES, 5 glucose, pH = 7.40, Osmolality = 310 mOsm. This mammalian photoreceptor Ringer's, lacking bicarbonate (but with a high concentration of HEPES), has been sufficient for obtaining and maintaining living mouse retinal slices. Isolated retinas were embedded in 3% low-temperature gelling agarose (gelling point 26°C) at 37°C, and then rapidly cooled to gel the agarose. The agarose blocks were sliced with vibratory microtome Vibratome 1000 (Vibratome Instruments, Saint Louis, MO) under dim red light. The slice thickness was typically 250 μm. Agarose slices containing the retinal slices were placed in a chamber that fit on the microscope stage. As judged by the metabolic competence for the reduction of all-*trans* retinal to all-*trans* retinol after bleaching, retinal slices can be kept alive at room temperature in this Ringer's for at least 6 h. During the course of the experiment, the slice was perfused with mammalian Ringer's.

Fluorescence imaging experiments on isolated frog rod photoreceptor cells were carried out on the stage of an inverted Zeiss Axiovert 100 microscope (Carl Zeiss, Thornwood, NY), using a Xenon continuous arc light source from Sutter Instrument Company (Novato, CA), a Zeiss 40× Plan Neofluar oil immersion objective lens (NA = 1.3), and a SensiCam CCD camera (Cooke Corporation, Auburn Hills, MI). The experiments were carried out at room temperature. Image acquisition and analysis were carried out using the Intelligent Imaging Innovations (Denver, CO) software. Rod outer segment and ellipsoid fluorescence was excited with 360 nm light and the emission was measured at 457 nm. In some experiments emission was also measured at 530 nm. The fluorescence intensity was measured over defined regions of interest (ROI) contained in the ellipsoid, the outer segment and background, and analyzed using the software. To allow for instrument-independent comparisons, the fluorescence intensities from the rod outer segment at different time points were normalized to the initial value of the fluorescence before bleaching. This normalization procedure did not introduce any spurious features, as neither the retinoic acid nor the inhibitors had a significant effect on the absolute value of the initial rod outer segment fluorescence. For fluorescence measurements of NADPH (see Fig. 3 *B*), the solution containing NADPH was placed in the same kind of chamber used for the measurements with cells.

Fluorescence imaging experiments on mouse retinal slices were carried out on the stage of an upright Zeiss Axioscope 2FS microscope (Carl Zeiss, Thornwood, NY), using a Till Photonics Monochromator light source (Eugene, OR), a Zeiss 40× Achroplan water immersion objective lens (NA = 0.8), and a SensiCam CCD camera (Cooke Corporation, Auburn Hills, MI). The experiments were carried out at room temperature. Image acquisition and analysis were carried out using the Intelligent Imaging Innovations (Denver, CO) software. Slice fluorescence was excited with 360 nm light and the emission was collected between 525 and 565 nm. The excitation light intensity did not cause significant bleaching of slice fluorescence. The fluorescence intensity was measured along the retinal layers using ImageJ software (http://rsb.info.nih.gov/ij/), allowing the separation of the fluorescence signal originating from different retinal layers. For this procedure to be valid, good vertical arrangement (stacking) of retinal layers in the slice was essential and was judged by focusing at different slice depths before imaging. Slices with inadequate layer stacking were discarded. To allow comparison across different slices and independent of instrument, the fluorescence intensities from the rod outer segment (ROS) layer at different time points were normalized to the initial value of the fluorescence before bleaching. As with the frog cell measurements, this normalization procedure did not introduce any spurious features, as the retinoic acid had no significant effect on the absolute value of the initial rod outer segment layer fluorescence.

Screening effects were an important concern in the experiments with mouse slices, which were imaged through a water-immersion lens in an upright microscope: in experiments where all-*trans* retinal was added there was a significant reduction of fluorescence (~36%) immediately after addition, presumably due to screening of the excitation light by the retinal-containing solution. The data after addition of all-*trans* retinal have been corrected for this effect through multiplication by a factor obtained by comparing the fluorescence intensity just before and immediately after the addition of all-*trans* retinal. For experiments with retinoic acid, there is no direct way to distinguish between screening and inhibition of retinol production. Therefore, we compared the screening effect of 100 μM all-*trans* retinal and 100 μM all-*trans* retinoic acid using fluorescence intensity calibration standards (2.5 μm diameter spheres having excitation/emission maxima at 350/440 nm from Molecular Probes, Eugene, OR) under the same optics and conditions as for experiments with slices. All-*trans* retinal reduced the measured fluorescence by ~16%, whereas all-*trans* retinoic acid reduced it by ~2%. If we extrapolate the sphere result to the slice, screening by retinoic acid should have no more than 5% of an effect on the fluorescence. Consistent with the lack of significant screening, the presence of retinoic acid had no detectable effect on the absolute value of the initial rod outer segment layer fluorescence. The lack of significant screening by retinoic acid (absorption maximum ~350 nm) as opposed to retinal (absorption maximum ~370 nm) is probably due to the cutting-off of the

lower wavelength light by the glass optics. In experiments with isolated frog rod photoreceptors, there was no possibility for screening, as they were carried out with an inverted microscope and the cell was imaged directly through the chamber's glass bottom using an oil immersion lens.

For two-photon microscopy, a Ti:Sapphire tunable IR laser was used to excite fluorescence (Williams et al., 1994) in bleached frog rods with 720 nm light through a Zeiss 40× water immersion lens (IR, NA = 0.8). The laser is part of a Zeiss LSM 510 Non-Linear Optical Confocal Microscope that includes an array of detectors for simultaneously measuring emission at different wavelengths (Zeiss 510 Meta system). The bandwidth for the emission measurements was 21.4 nm at each wavelength.

All reagents were of analytical grade. Bovine serum albumin (BSA) was dissolved in Ringer's at 1% (150 μM) concentration. All-*trans* retinal, all-*trans* retinol, and retinoic acid were dissolved in ethanol and their concentrations measured with a spectrophotometer. All-*trans* retinal and all-*trans* retinol were delivered to the cells using 1% BSA as carrier. No carrier was used for retinoic acid. For the inhibition experiments, isolated cells or slices were preincubated for 15 min with retinoic acid before the initial measurement. This preincubation time was chosen as it is the time it takes exogenous all-*trans* retinol to equilibrate. All experiments were carried out at room temperature.

RESULTS

Bleaching of rhodopsin in an isolated dark-adapted frog rod photoreceptor leads to the gradual increase in fluorescence in the outer segment (Fig. 1), similar to what has been observed in salamander rods (Tsina et al., 2004). Fig. 1 *A* shows a bright field infrared image of an isolated frog rod. The cell is dark-adapted and in the first fluorescence image (Fig. 1 *B*) most of the fluorescence is concentrated in the ellipsoid region of the cell, which is densely packed with mitochondria. The dark-adapted outer segment shows a very small level of fluorescence. Subsequently, the cell was exposed for 1 min to intense 490 nm light from the Xenon light source that bleached almost the full complement of the outer segment rhodopsin. The image acquired immediately after the end of the bleach showed a slight increase in outer segment fluorescence (Fig. 1 *C*). Subsequently, images were acquired every 5 min, and showed a steady increase in outer segment fluorescence (Fig. 1, *D* and *E*). To quantify the fluorescence changes occurring in the outer segment after rhodopsin bleaching and allow comparisons across instruments and cells with outer segments of different diameters, the value of the outer segment fluorescence at each time point was divided by the initial value before bleaching. The solid circles in Fig. 1 *F* show the averaged data from 12 rods. The initial value before bleaching (at $t = -1$ min) is 1 due to the normalization. Immediately after bleaching (at $t = 0$ min) outer segment fluorescence has increased, and continues increasing reaching a maximum after 30–40 min; then it begins to decline slowly. The decline does not reflect fluorophore bleaching, as control experiments showed that each measurement bleached <0.5% of the fluorophore.

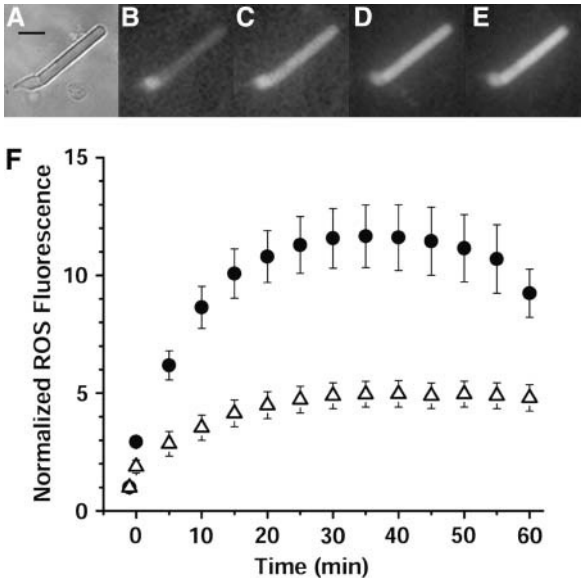

FIGURE 1 Production of retinol after rhodopsin bleaching in isolated frog rod photoreceptors. (*A*) Infrared image of a dark-adapted isolated frog rod. Bar is 10 μm. (*B–E*) Fluorescence images (excitation, 360 nm; emission, 457 nm) of the rod in *A* at various time points: (*B*) Dark-adapted cell, before exposure to light; (*C*) immediately after exhaustive bleaching of rhodopsin for 1 min; (*D*) 10 min after bleaching; (*E*) 30 min after bleaching; and (*F*) increase of outer segment fluorescence with time after rhodopsin bleaching. The first time point (at $t = -1$ min) is the outer segment fluorescence of the dark-adapted cell. All subsequent fluorescence values have been normalized to this one. (●) averaged data from 12 cells under control conditions; (△) averaged data from six cells in the presence of 100 μM retinoic acid, a retinol dehydrogenase inhibitor. Retinoic acid suppresses the increase in fluorescence.

The fluorescence increase in the outer segment after bleaching has been observed before and attributed to the all-*trans* retinol produced from the reduction of the all-*trans* retinal released from photostimulated rhodopsin (Kaplan, 1985; Tsina et al., 2004). Carrying out the bleaching in the presence of 100 μM retinoic acid, a retinol dehydrogenase inhibitor (Palczewski et al., 1994), resulted in marked suppression of the fluorescence increase ($n = 6$; Fig. 1 *F*, *open triangles*). However, the inhibition did not increase the time it took for the outer segment fluorescence to rise to a steady-state level. The suppression of fluorescence was not an artifact of the normalization procedure, as retinoic acid did not affect the absolute value of the initial rod outer segment fluorescence.

The results of Fig. 1 show that there is also significant fluorescence in the ellipsoid region of the cell, as has been observed before (Kaplan, 1985; Tsina et al., 2004). As the ellipsoid is rich in mitochondria, this fluorescence may be due to reduced pyridine nucleotides, NADH, and NADPH (Chance and Thorell, 1959). NADH and NADPH have identical fluorescence excitation and emission spectra (Patterson et al., 2000) and are subsequently referred to as NAD(P)H. Fig. 2 shows that the emission spectrum of the ellipsoid fluorescence is different from that of the outer segment fluorescence, consistent with different fluorophores being responsible. Fluorescence was excited with 720 nm light (two-photon molecular excitation), and the emission was measured at different wavelengths between 409 and 644 nm.

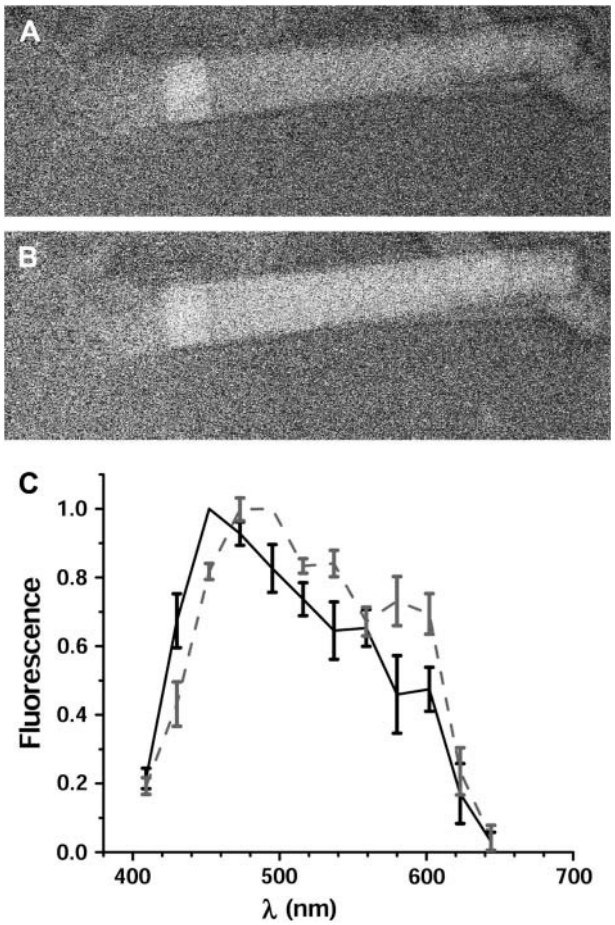

FIGURE 2 Different origin of the fluorescence in the ellipsoid and the outer segment regions of a rod photoreceptor. Fluorescence was excited with 720 nm light from a Ti:Sapphire laser. (*A*) Fluorescence image at emission 430 nm (21.4 nm bandwidth, centered at 430 nm). The ellipsoid fluorescence is strongest and clearly visible. (*B*) Fluorescence image at emission 473 nm (21.4 nm bandwidth). The outer segment fluorescence intensity is similar to that from the ellipsoid region. (*C*) Emission spectra from ellipsoid (*black solid line*) and outer segment (*shaded dashed line*), from $n = 6$ rod cells. The straight-line segments connect the experimental points. Error bars represent standard errors.

Fig. 2 *A* shows the fluorescence image of a bleached frog rod measured at 430 nm. The ellipsoid region is the brightest. Fig. 2 *B* shows the fluorescence image of the same rod measured at 473 nm. At this emission wavelength, the outer segment and the ellipsoid regions have similar brightness, suggesting that the fluorophore in the outer segment is different from that in the ellipsoid. The fluorescence emission spectra from the outer segment and the ellipsoid region are shown in Fig. 2 *C* ($n = 6$ rod cells). Fluorescence values for the ellipsoid were normalized to the value at 452 nm, whereas the values in the outer segment were normalized to the value at 495 nm. As expected from the images in Fig. 2, *A* and *B*, the fluorescence emission spectrum for the outer segment is red-shifted compared to that for the ellipsoid, again suggesting that different fluorophores are responsible.

The all-*trans* retinol fluorescence emission spectrum is indeed red-shifted with respect to that of NADPH (Fig. 3 *A*). The emission spectrum is not a mirror image of the absorption spectrum, presumably because of the contribution from a low-lying and weakly allowed electronic state ($^1A_g^-$) that is distinct from the main absorption band transition state (^1B_u) (see review by Honig and Ebrey, 1974 for discussion). This red shift should result in different relative emissions at different wavelengths. To confirm the identity of the fluorophores responsible for the fluorescence from the ellipsoid and outer segment compartments, we compared the emission

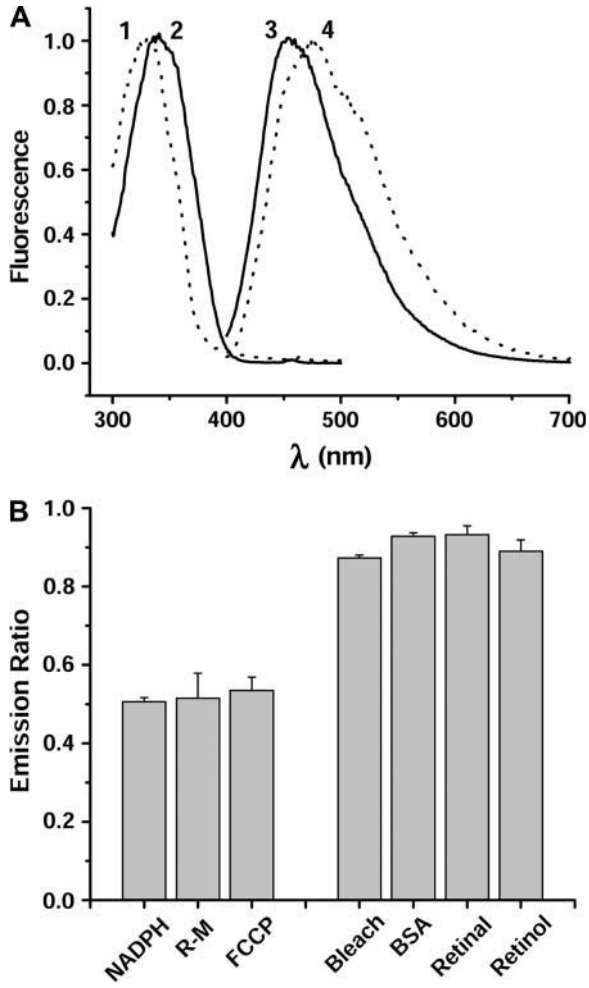

FIGURE 3 (*A*) Fluorescence excitation and emission spectra obtained in a spectrofluorimeter. (*1*) Retinol excitation, (*2*) NADPH excitation, (*3*) NADPH emission, and (*4*) retinol emission. (*B*) 530:457 emission ratios for fluorescence intensity changes under different treatments. NADPH in chamber ($n = 6$); R-M, ellipsoid fluorescence increase after rotenone + myxothiazole ($n = 4$); FCCP, ellipsoid fluorescence decrease after FCCP ($n = 8$); bleach, outer segment fluorescence increase 30 min after exhaustive bleach ($n = 7$); BSA, outer segment fluorescence decrease 30 min after exposure to 1% BSA ($n = 7$); retinal, outer segment fluorescence increase 15 min after addition of 100 μM retinal ($n = 5$); retinol, outer segment fluorescence increase 15 min after addition of 100 μM retinol ($n = 6$). Error bars represent standard errors.

ratios at 530 and 457 nm for the fluorescence changes brought about by a variety of experimental manipulations (Fig. 3 *B*). Rotenone and myxothiazole are inhibitors of the mitochondrial electron transport chain and lead to accumulation of NADH (Halangk and Kunz, 1991). Exposure of rod photoreceptors to 5 μM rotenone and 2 μM myxothiazole led to a fluorescence increase in the mitochondrial (ellipsoid) region. The F_{530}/F_{457} emission ratio for this fluorescence increase was indistinguishable from the ratio for NADPH. FCCP on the other hand is an uncoupler of oxidative phosphorylation and leads to the exhaustion of NADH and the accumulation of the nonfluorescent NAD^+ (Halangk and Kunz, 1991). Exposure of rod photoreceptors to 10 μM FCCP resulted in a decrease in fluorescence in the ellipsoid region. This fluorescence decrease also had a F_{530}/F_{457} emission ratio indistinguishable from the ratio for NADPH. Addition of exogenous all-*trans* retinol led to a fluorescence increase in the outer segment as the retinol accumulated in the rod disk membranes, and made it possible to obtain the F_{530}/F_{457} emission ratio for retinol fluorescence. The rod outer segment fluorescence increase measured 30 min after the bleaching of rhodopsin had the same F_{530}/F_{457} emission ratio as all-*trans* retinol. Incubation with 150 μM BSA for 30 min led to a reduction in the ROS fluorescence, with F_{530}/F_{457} emission ratio the same as all-*trans* retinol, consistent with the lipophilic fluorophore removed by BSA being retinol. Finally, addition of exogenous all-*trans* retinal led to a ROS fluorescence increase with the same F_{530}/F_{457} emission ratio as all-*trans* retinol, suggesting that the exogenously supplied retinal is reduced to retinol by the retinol dehydrogenase. In summary, the results of Fig. 3 *B* show that the fluorescence signal from the ellipsoid region is consistent with NAD(P)H, whereas that from the outer segment region is consistent with all-*trans* retinol.

Since the reduction of all-*trans* retinal to retinol requires NADPH, suppression of metabolic activity should also suppress the reduction. Metabolic pathways that can supply the required NADPH in the cytoplasm include the pentose phosphate pathway (Hsu and Molday, 1994) and $NADP^+$-linked isocitrate and malate dehydrogenases (Winkler, 1986) utilizing substrates provided by the mitochondria. NADPH can also be synthesized from NADH by transhydrogenases. To suppress metabolic activity, we have employed three inhibitory cocktails that: a), inhibit glycolysis and the pentose phosphate pathway; b), deplete mitochondrial NAD(P)H pools and also stop mitochondrial generation of ATP; and c), inhibit the mitochondrial tricarboxylate transporter. Application of all of these a), b), and c) treatments together significantly suppressed the rise in ROS fluorescence after bleaching (Fig. 4 *A*, *open triangles*), in agreement with the reduction of all-*trans* retinal to retinol being responsible for the increase in fluorescence. As in the case of inhibition of the reduction by retinoic acid, the treatment did not increase the time it took for the outer segment fluorescence reach a steady-state level. As before, the suppression of fluorescence was not an artifact of the normalization procedure, as the inhibitors did not have a significant effect on the absolute value of the initial rod outer segment fluorescence.

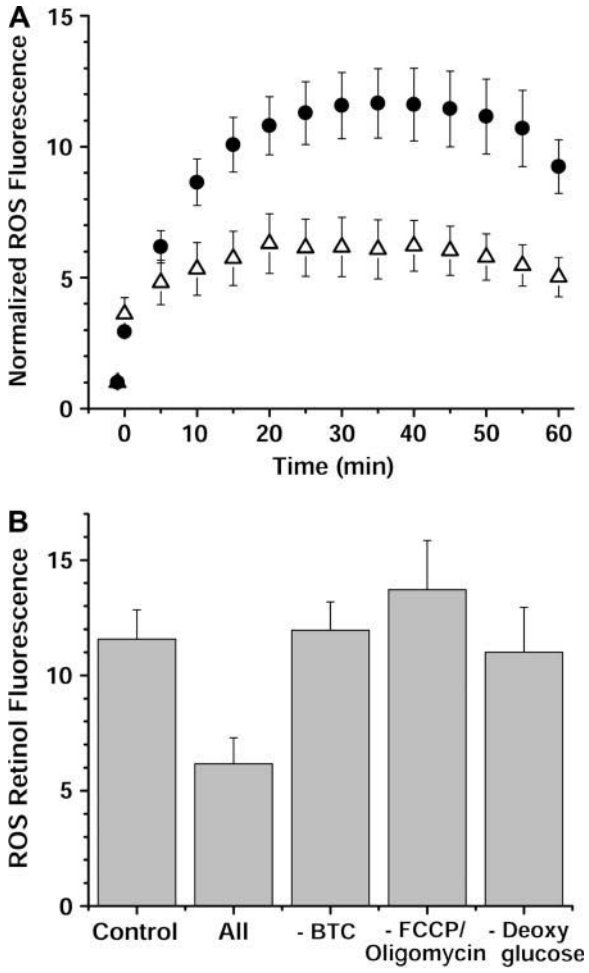

FIGURE 4 Effects of metabolic inhibitors on production of all-*trans* retinol after bleaching. (*A*) Control (●) and all the inhibitors together (△). Error bars represent standard errors. (*B*) All the inhibitors are needed for the effect. Outer segment fluorescence 30 min after exhaustive bleach in the presence of different inhibitory cocktails. The cell numbers were: control, $n = 12$; all inhibitors, $n = 9$; without 1,2,3-BTC, $n = 6$; without FCCP and oligomycin, $n = 7$; without deoxyglucose, $n = 7$. Error bars represent standard errors.

We further quantified the effect of metabolic suppression by comparing the levels of ROS fluorescence reached at 30 min after bleaching. We found that removal of any one of the three inhibitory treatments resulted in the rescue of the fluorescence increase (Fig. 4 *B*). Also, substitution of the inactive isomer 1,2,4-BTC (Cheema-Dhadli et al., 1976) for 1,2,3-BTC had no effect on all-*trans* retinol formation: the normalized fluorescence at 30 min was 10.4 ± 1.0 ($n = 8$) for 1,2,4-BTC plus the a) and b) treatments, whereas it was 11.6 ± 1.3 ($n = 12$) for control, 12.0 ± 1.2 ($n = 6$) for the a) and b) treatments without 1,2,3-BTC, and 6.2 ± 1.1 ($n = 9$) for a), b), and c) treatments together. Therefore, the effect of 1,2,3-BTC was specific. The results indicate that the cells

can utilize NADPH produced from different metabolic pathways, and it is only upon suppression of several pathways simultaneously that NADPH becomes limiting. The results further suggest that the frog rod cells contain significant stores of metabolites that the cell can draw upon to maintain metabolic activity even in the absence of primary substrate (glucose) and under inhibition of other metabolic pathways.

Mouse rods are much smaller and more fragile than amphibian rods, and we have not been able to consistently obtain viable preparations of isolated mouse rods. We addressed this problem by using a slice preparation from mouse retinas that proved to be very robust for following the reduction of all-*trans* retinal to retinol. Fig. 5 shows a biochemically active 250-μm thick retinal slice from a C57BL/6 mouse. Panel *A* is a Nomarski image, showing the retinal layers with the photoreceptor outer segments at the top of the slice. Panel *B* is a fluorescence image of the same field, obtained with 360 nm excitation and >500 nm emission filters. This is a bleached retina and the fluorescence in the rod outer segments is due to all-*trans* retinol that is produced from the reduction of the all-*trans* retinal generated upon bleaching. It is not clear what the fluorescence from the other layers originates from, but NADH and NADPH may be contributing to it. Experiments with mouse retinal slices were carried out at room temperature allowing a direct comparison with the frog results.

Fig. 6 shows an experiment with a retinal slice from a C57BL/6 mouse. Panel *A* is a Nomarski image of the ROS area of the slice, taken with infrared light at the beginning of the experiment. Panels *B–E* show the fluorescence images of the same field, obtained with 360 nm excitation and 525–565 nm emission filters. Panel *B* is the first fluorescence image of the unbleached slice. Panel *C* is the first fluorescence image obtained immediately after bleaching the slice with white light. Panels *D* and *E* are the images obtained 10 min and 90 min after bleaching, respectively. Panel *F* shows the fluorescence profiles of the images (*B–E*) along the length of the photoreceptor layer. There is a large progressive increase in fluorescence in the ROS layer after bleaching, reflecting the reduction of all-*trans* retinal (generated from rhodopsin bleaching) to all-*trans* retinol. The accompanying increase in fluorescence in the RIS layer may be due to NAD(P)H, reflecting stimulation of mitochondrial metabolic activity.

To quantify the fluorescence changes occurring in mouse ROS after rhodopsin bleaching, similar experimental and data analysis procedures as with frog rods were followed: images were acquired every 5 min, and the value of the outer segment layer fluorescence at each time point was divided by the initial value before bleaching. The solid circles in Fig. 7 show the averaged data from 10 slices. The initial value before bleaching (at $t = -1$ min) is normalized to 1. Immediately after bleaching (at $t = 0$ min) outer segment fluorescence has increased, and continues increasing reaching a maximum after ~60 min. As in the case of frog rods, carrying out the bleaching in the presence of 100 μM of the retinol dehydrogenase inhibitor retinoic acid (Palczewski et al., 1994) resulted in marked suppression of the fluorescence increase ($n = 5$ slices; Fig. 7, *open squares*), whereas not increasing the time it takes fluorescence to reach steady state. ROS layer fluorescence increased after addition of 100 μM all-*trans* retinal ($n = 5$ slices; Fig. 7, *open triangles*), indicating that mouse rod outer segments reduce exogenously added all-*trans* retinal. No significant fluorescence changes were observed after addition of 9-*cis* or 11-*cis* retinals, indicating that these isomers were not readily reduced, in accordance with the known stereospecificity of the dehydrogenase (Palczewski et al., 1994).

To further test the notion that the fluorescence increase in rod outer segments after rhodopsin bleaching is due to all-*trans* retinol, we repeated the experiments with slices from the retinas of *Rpe*65$^{-/-}$ mice (Fig. 8, *A–E*). The Visual Cycle is impaired in these mice and the retinas lack 11-*cis* retinal and rhodopsin (Redmond et al., 1998). No significant fluorescence increases were observed in the rod outer segments of *Rpe*65$^{-/-}$ mice after bleaching (Fig. 8 *F*, *solid circles*), in agreement with the absence of significant amounts of visual pigment in these cells (Redmond et al., 1998; but see Fan et al., 2003 and discussion below). Addition of all-*trans* retinal resulted in an increase in rod outer segment fluorescence similar to the one observed in wild-type mice (Fig. 8 *F*, *open triangles*), suggesting that the dehydrogenase step is not compromised in the *Rpe*65$^{-/-}$ animals.

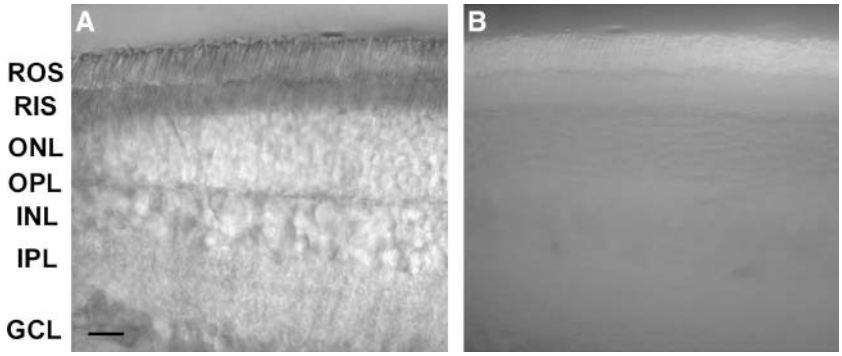

FIGURE 5 A biochemically active slice from a mouse retina. (*A*) Nomarski image. Abbreviations: ROS, rod outer segments; RIS, rod inner segments (the photoreceptor ellipsoids); ONL, outer nuclear layer; OPL, outer plexiform layer; INL, inner nuclear layer; IPL, inner plexiform layer; and GCL, ganglion cell layer. (*B*) Fluorescence image of the field in *A*. Scale bar is 10 μm. The experiment was carried out at room temperature.

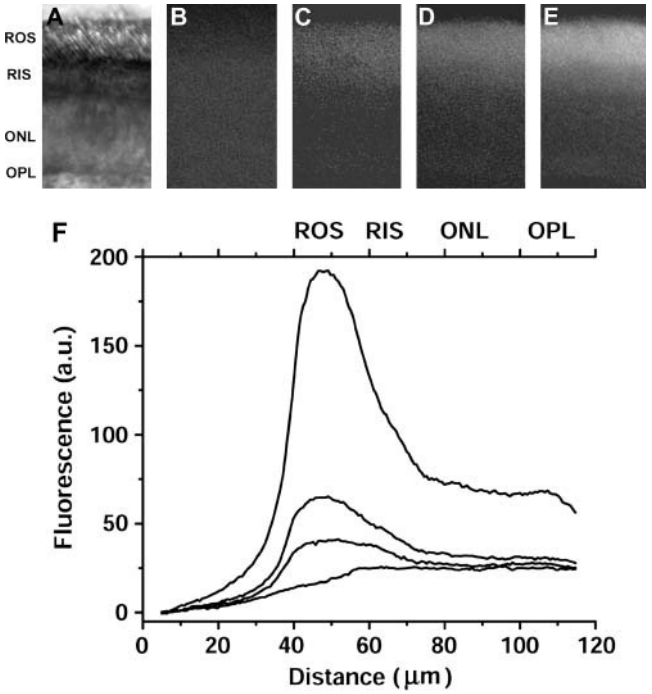

FIGURE 6 Generation of all-*trans* retinol in a wild-type mouse retinal slice after bleaching. The panels show the photoreceptor layer of the slice. (*A*) Infrared image of the photoreceptor layer of an unbleached retinal slice. (*B*) Slice fluorescence before bleaching. (*C–E*) Fluorescence after bleaching: (*C*) Immediately after, (*D*) after 10 min, and (*E*) after 90 min. (*F*) Fluorescence profiles of the images (*B–E*) along the length of the photoreceptor layer. The rod outer segment layer fluorescence increases from *B* to *E*. Experiments were carried out at room temperature.

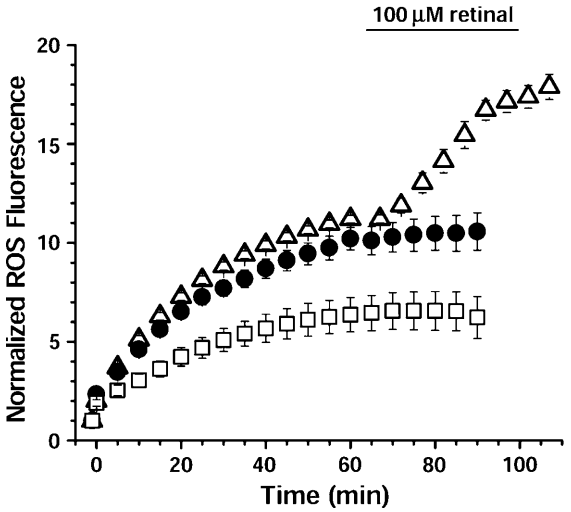

FIGURE 7 Increase of outer segment fluorescence with time after rhodopsin bleaching. The first time point (at $t = -1$ min) is the outer segment fluorescence of the dark-adapted slice. All subsequent fluorescence values have been normalized to this one. (●) Control ($n = 10$); (□) in the presence of 100 μM retinoic acid, a retinol dehydrogenase inhibitor ($n = 5$); and (△) addition of 100 μM all-*trans* retinal 60 min after bleaching ($n = 5$). Experiments were carried out at room temperature.

DISCUSSION

After bleaching of the visual pigment rhodopsin, there is a large fluorescence increase in the outer segments of rod photoreceptors. This fluorescence is of a different origin than the fluorescence of the mitochondria-rich ellipsoid region of the cell, which is due to NAD(P)H. The outer segment fluorescence is due to the appearance of all-*trans* retinol, produced from the reduction of all-*trans* retinal that is released after rhodopsin bleaching. It is not due to retinyl esters, as they do not appear to form in the outer segment (Zimmerman, 1974; Bridges, 1976). It takes 30–40 min after bleaching for the level of all-*trans* retinol to reach a maximum in frog rods, in close agreement with measurements in salamander rods (Tsina et al., 2004). As the fluorescence reaches a maximum in 60 min in mouse rods at room temperature, it appears that the formation of all-*trans* retinol proceeds with similar kinetics in different species. The level of rod outer segment retinol concentration, as manifested by its fluorescence, reflects a balance between its formation and its removal. This slow removal is evidenced by the slow decline of fluorescence in frog rods after ~40 min. In the presence of lipophilic carrier proteins the removal is accelerated (see Tsina et al., 2004). The retinol removal is probably due to slow partitioning into the bulk aqueous solution, though we cannot exclude the possibility of retinol diffusing and getting trapped in the form of retinyl esters in other photoreceptor cell compartments (Zimmerman, 1974; Bridges, 1976). Consistent with a balance between retinol formation and removal, inhibition of the formation of retinol by retinoic acid or metabolic inhibitors suppresses the maximal level of concentration that is reached. So, the concentration of retinol present in the outer segment does not reflect the total amount of retinol formed.

The broadly similar kinetics of the retinol fluorescence increase after bleaching across species could be considered rather surprising. Mouse rods are ~100× smaller than amphibian rods and contain a proportionately smaller number of visual pigment molecules, which would mean that less NADPH is required for the reduction of the all-*trans* retinal produced by the bleaching. Since the metabolic activity of mouse rods may be expected to be different from that of amphibian rods, this broad kinetic agreement could be fortuitous. But it could also be an indication that steps other than the reduction of all-*trans* retinal are kinetically important (see below).

The slow kinetics of retinol formation is consistent with the reduction of all-*trans* retinal being the rate-limiting step in the Visual Cycle, as proposed by Saari (2000) on the basis of experiments with whole animals (Saari et al., 1998) and by Tsina et al. (2004) on the basis of experiments with isolated salamander rods. In further agreement with this notion, inhibition of retinol dehydrogenase with retinoic acid, and suppression of metabolic activity, which would lower the NADPH levels, resulted in significant reduction of the concentration of all-*trans* retinol reached. However, these treatments did not slow down the rate at which retinol formation

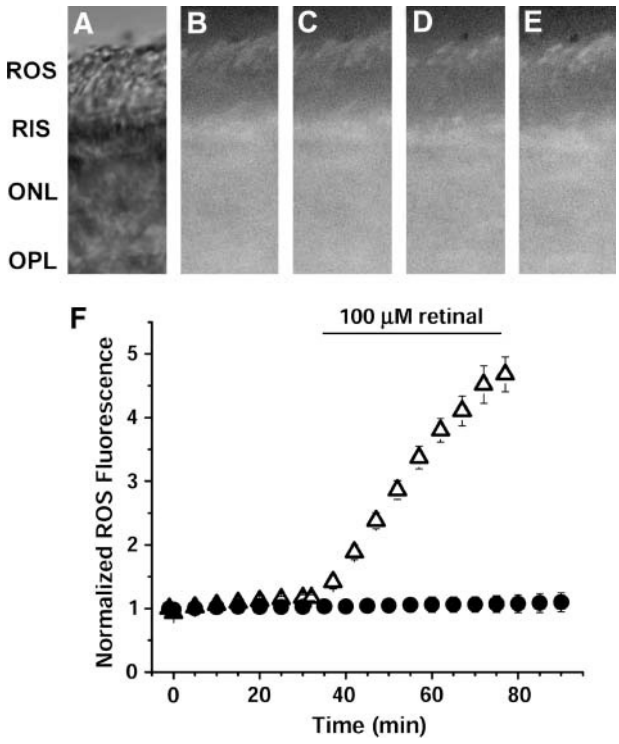

FIGURE 8 Fluorescence changes reflecting all-*trans* retinol production in the rod outer segments of *Rpe*65$^{-/-}$ mice. The panels show the photoreceptor layer of the slice. (*A*) Infrared image of the photoreceptor layer of an unbleached retinal slice. (*B*) Slice fluorescence before bleaching. (*C–E*) Fluorescence after bleaching: (*C*) Immediately after, (*D*) after 10 min, and (*E*) after 90 min. *(F)* Kinetics of fluorescence change. The ROS fluorescence was measured from the fluorescence profiles obtained at different times after bleaching and delivery of all-*trans* retinal. Bleaching took place between time $t = -1$ min and $t = 0$. The first time point (at $t = -1$ min) is the outer segment fluorescence of the dark-adapted slice. All subsequent fluorescence values have been normalized to this one. (●) Control ($n = 6$); (△) addition of 100 μM all-*trans* retinal 30 min after bleaching ($n = 6$). Experiments were carried out at room temperature.

reached a steady state. If the retinol dehydrogenase reaction were the only slow step in the production of retinol, then the effects of the inhibitory treatments would include also a slow down of the rate at which retinol formation reached a steady state. Therefore, the data indicate that there must be more slow steps involved, steps that occur earlier than the retinol dehydrogenase reaction. One possibility for such a slow step is the release of all-*trans* retinal from the opsin binding site, which could take several minutes (Matthews et al., 1963; Farrens and Khorana, 1995; Shichida and Imai, 1999). Another possibility is the transport of all-*trans* retinal from the opsin to the retinol dehydrogenase: after release from opsin, all-*trans* retinal is reversibly bound to phosphatidylethanolamine inside the disks, and is subsequently transported to the cytosol and made available to retinol dehydrogenase by the ABCR protein (Weng et al., 1999). Mutations in the ABCR protein are responsible for Stargardt's disease, an early onset form of macular degeneration. The presence of additional slow steps before the retinol dehydrogenase would be consistent with the results of Saari et al. (1998) and those of Tsina et al. (2004). It is important to keep in mind that in isolated cells and tissues there is no mechanism for the rapid removal of the generated all-*trans* retinol, in contrast to the situation in the whole animal. Thus, all-*trans* retinol accumulates in the ROS and reaches higher concentrations, a feature that allows the monitoring of the reduction reaction, but also presents an important difference with the in vivo situation. The two treatments, inhibition of retinol dehydrogenase and suppression of metabolic activity, both result in a reduction in the maximal level of all-*trans* retinol that is reached after bleaching. As described above, this is consistent with the maximal levels of retinol attained reflecting a balance between production from the reduction of all-*trans* retinal and loss from the outer segment membranes to extracellular space. This balance is achieved after the completion of the prior slow steps that dominate the overall kinetics.

In frog rods, the formation of all-*trans* retinol after bleaching is suppressed by a combination of metabolic inhibitors. These inhibitors are expected to suppress the different metabolic pathways that synthesize the NADPH necessary for the reduction of all-*trans* retinal, and the combination reduces the mitochondrial NAD(P)H fluorescence. Since it is not certain that each of these inhibitors would work as expected in an intact cell, it is the actual observation of the suppression of retinol formation that serves as a positive control. The inhibitors are targeting a), glycolysis and the pentose phosphate pathway; b), mitochondrial ATP and NAD(P)H generation; and c), mitochondrial isocitrate transport. If any of these three pathways is allowed to function unperturbed, the retinol formation is unaffected. The results suggest that multiple pathways can contribute to the generation of the NADPH necessary for the reduction of all-*trans* retinal. These data are consistent with the pentose phosphate pathway (Hsu and Molday, 1994) as well as with $NADP^+$-linked isocitrate dehydrogenase (Winkler, 1986) being able to supply the reducing equivalents. The mitochondrial contribution is clearly not limited to ATP, which could be used for the phosphorylation of glucose, but may also include isocitrate and other metabolites. A surprising result is that the inhibition of glucose phosphorylation is not sufficient by itself to suppress the production of NADPH. Since glucose is the primary metabolic substrate for the mitochondrial metabolism as well, this suggests that the cells contain sufficient stores of metabolites that they can draw upon, a conclusion consistent with the presence of glycogen stores (Witkovsky and Yang, 1982; Fliesler et al., 1997). The presence of such stores is probably a feature of amphibian neurons. Preliminary experiments in mouse retinal slices (Chen, Solessio, Barlow, and Koutalos, unpublished observations) indicate that the mere removal of glucose reversibly suppresses the formation of all-*trans* retinol in rod outer segments after rhodopsin bleaching. This observation is consistent with the lack of metabolite stores in mammalian rod photoreceptors (Rungger-Brandle

et al., 1996). However, even in the mouse, the metabolic pathways that provide the NADPH required for retinol formation appear to be quite robust. Thus, retinol formation proceeds at room temperature, when under similar conditions the light-sensitive current of mammalian rod photoreceptors becomes almost undetectable (Robinson et al., 1993). The situation also contrasts with the metabolic sensitivity of retinol-processing steps in the retinal pigment epithelium that seem to be responsible for the blocking of the visual cycle in excised mouse eyes (Ostroy et al., 1993; Palczewski et al., 1999).

The rod photoreceptors of *Rpe*65$^{-/-}$ mice have been shown to contain small amounts of isorhodopsin, a 9-*cis* retinal containing pigment (Fan et al., 2003), which is responsible for light responses obtained from these photoreceptors. The amount of isorhodopsin in *Rpe*65$^{-/-}$ animals that have been kept in the dark for 5 weeks reaches ~5% of the wild-type pigment level (Fan et al., 2003), but is quickly lost when the animal is exposed to cyclic light. In the experiments reported here, the animals were kept in cyclic light, and were not dark-adapted for more than a few hours before the experiment. The observed lack of a significant increase in rod outer segment fluorescence after bleaching is therefore consistent with the lack of a significant amount of rhodopsin or isorhodopsin present. As retinol formation proceeds briskly upon addition of exogenous all-*trans* retinal, it appears that in these genetically modified animals the retinol dehydrogenase step is not affected and the rod photoreceptors remain metabolically competent.

In conclusion, we have established that the fluorescence signals from the outer segment and from the ellipsoid region of rod photoreceptors are due to all-*trans* retinol and NAD(P)H, respectively. We find that at room temperature the formation of all-*trans* retinol after rhodopsin bleaching is slow, taking 30–60 min to reach maximum level in an amphibian and a mammalian species. The data presented here are consistent with additional slow steps occurring before the reduction of all-*trans* retinal by retinol dehydrogenase. In frog rods, the NADPH required for the formation of all-*trans* retinol can be supplied from multiple metabolic pathways. Finally, we used the genetically modified *Rpe*65$^{-/-}$ mice to demonstrate that no significant rod outer segment fluorescence changes are observed after bleaching in the absence of 11-*cis* retinal.

We thank Dr. Michael Redmond for making the *Rpe*65$^{-/-}$ mice available to us, Dr. Fred Rieke for generous advice regarding the mouse retinal slice preparation, Dr. Masahiro Kono for helpful discussions, and Dr. Judson Chandler for help with two-photon microscopy.

The Zeiss LSM 510 Non-Linear Optical Confocal Microscope is part of a core facility at the Medical University of South Carolina (MUSC) (supported by 1S10RR015776). This work was supported by Human Frontier Science Program grant RG0204/2000-B (Y.K.), National Institutes of Health Grants DA10266 (S.V.), EY01157 (M.C.C.), EY04939 (R.K.C.), EY014850 (Y.K.), and EY014793, Foundation Fighting Blindness (M.C.C. and R.K.C.), and an unrestricted grant to MUSC from Research to Prevent Blindness (RPB), New York, NY. R.K.C. is an RPB Senior Scientific Investigator.

REFERENCES

Adler, A. J., and R. B. Edwards. 2000. Human interphotoreceptor matrix contains serum albumin and retinol-binding protein. *Exp. Eye Res.* 70: 227–234.

Bernstein, P. S., and R. R. Rando. 1986. In vivo isomerization of all-*trans*- to 11-*cis*-retinoids in the eye occurs at the alcohol oxidation state. *Biochemistry.* 25:6473–6478.

Biernbaum, M. S., and M. D. Bownds. 1985. Frog rod outer segments with attached inner segment ellipsoids as an in vitro model for photoreceptors on the retina. *J. Gen. Physiol.* 85:83–105.

Bridges, C. D. 1976. Vitamin A and the role of the pigment epithelium during bleaching and regeneration of rhodopsin in the frog eye. *Exp. Eye Res.* 22:435–455.

Chance, B., and B. Thorell. 1959. Localization and kinetics of reduced pyridine nucleotide in living cells by microfluorimetry. *J. Biol. Chem.* 234:3044–3050.

Cheema-Dhadli, S., B. H. Robinson, and M. L. Halperin. 1976. Properties of the citrate transporter in rat heart: implications for regulation of glycolysis by cytosolic citrate. *Can. J. Biochem.* 54:561–565.

Ebrey, T., and Y. Koutalos. 2001. Vertebrate photoreceptors. *Prog. Retin. Eye Res.* 20:49–94.

Fain, G. L., H. R. Matthews, M. C. Cornwall, and Y. Koutalos. 2001. Adaptation in vertebrate photoreceptors. *Physiol. Rev.* 81:117–151.

Fan, J., B. Rohrer, G. Moiseyev, J. X. Ma, and R. K. Crouch. 2003. Isorhodopsin rather than rhodopsin mediates rod function in RPE65 knock-out mice. *Proc. Natl. Acad. Sci. USA.* 100:13662–13667.

Farrens, D. L., and H. G. Khorana. 1995. Structure and function in rhodopsin. Measurement of the rate of metarhodopsin II decay by fluorescence spectroscopy. *J. Biol. Chem.* 270:5073–5076.

Fliesler, S. J., M. J. Richards, C. Y. Miller, S. McKay, and B. S. Winkler. 1997. In vitro metabolic competence of the frog retina: effects of glucose and oxygen deprivation. *Exp. Eye Res.* 64:683–692.

Futterman, S., A. Hendrickson, P. E. Bishop, M. H. Rollins, and E. Vacano. 1970. Metabolism of glucose and reduction of retinaldehyde in retinal photoreceptors. *J. Neurochem.* 17:149–156.

Halangk, W., and W. S. Kunz. 1991. Use of NAD(P)H and flavoprotein fluorescence signals to characterize the redox state of pyridine nucleotides in epididymal bull spermatozoa. *Biochim. Biophys. Acta.* 1056: 273–278.

He, L., A. T. Poblenz, C. J. Medrano, and D. A. Fox. 2000. Lead and calcium produce rod photoreceptor cell apoptosis by opening the mitochondrial permeability transition pore. *J. Biol. Chem.* 275:12175–12184.

Honig, B., and T. G. Ebrey. 1974. The structure and spectra of the chromophore of the visual pigments. *Annu. Rev. Biophys. Bioeng.* 3:151–177.

Hoppe, J., D. Gatti, H. Weber, and W. Sebald. 1986. Labeling of individual amino acid residues in the membrane-embedded F0 part of the F1 F0 ATP synthase from Neurospora crassa. Influence of oligomycin and dicyclohexylcarbodiimide. *Eur. J. Biochem.* 155:259–264.

Hsu, S. C., and R. S. Molday. 1994. Glucose metabolism in photoreceptor outer segments. Its role in phototransduction and in NADPH-requiring reactions. *J. Biol. Chem.* 269:17954–17959.

Kaplan, M. W. 1985. Distribution and axial diffusion of retinol in bleached rod outer segments of frogs (*Rana pipiens*). *Exp. Eye Res.* 40:721–729.

Kletzien, R. F., and J. F. Perdue. 1973. The inhibition of sugar transport in chick embryo fibroblasts by cytochalasin B. Evidence for a membrane-specific effect. *J. Biol. Chem.* 248:711–719.

Koutalos, Y., K. Nakatani, T. Tamura, and K. W. Yau. 1995. Characterization of guanylate cyclase activity in single retinal rod outer segments. *J. Gen. Physiol.* 106:863–890.

Mata, N. L., R. A. Radu, R. C. Clemmons, and G. H. Travis. 2002. Isomerization and oxidation of vitamin a in cone-dominant retinas: a novel pathway for visual-pigment regeneration in daylight. *Neuron*. 36: 69–80.

Matthews, R. G., R. Hubbard, P. K. Brown, and G. Wald. 1963. Tautomeric forms of metarhodopsin. *J. Gen. Physiol*. 47:215–240.

McBee, J. K., V. Kuksa, R. Alvarez, A. R. de Lera, O. Prezhdo, F. Haeseleer, I. Sokal, and K. Palczewski. 2000. Isomerization of all-*trans*-retinol to *cis*-retinols in bovine retinal pigment epithelial cells: dependence on the specificity of retinoid-binding proteins. *Biochemistry*. 39: 11370–11380.

Nakatani, K., C. Chen, and Y. Koutalos. 2002. Calcium diffusion coefficient in rod photoreceptor outer segments. *Biophys. J*. 82:728–739.

Okajima, T. I., D. R. Pepperberg, H. Ripps, B. Wiggert, and G. J. Chader. 1990. Interphotoreceptor retinoid-binding protein promotes rhodopsin regeneration in toad photoreceptors. *Proc. Natl. Acad. Sci. USA*. 87: 6907–6911.

Ostroy, S. E., C. G. Gaitatzes, and A. L. Friedmann. 1993. Hypoxia inhibits rhodopsin regeneration in the excised mouse eye. *Invest. Ophthalmol. Vis. Sci*. 34:447–452.

Palczewski, K., S. Jager, J. Buczylko, R. K. Crouch, D. L. Bredberg, K. P. Hofmann, M. A. Asson-Batres, and J. C. Saari. 1994. Rod outer segment retinol dehydrogenase: substrate specificity and role in phototransduction. *Biochemistry*. 33:13741–13750.

Palczewski, K., J. P. Van Hooser, G. G. Garwin, J. Chen, G. I. Liou, and J. C. Saari. 1999. Kinetics of visual pigment regeneration in excised mouse eyes and in mice with a targeted disruption of the gene encoding interphotoreceptor retinoid-binding protein or arrestin. *Biochemistry*. 38:12012–12019.

Parlo, R. A., and P. S. Coleman. 1986. Continuous pyruvate carbon flux to newly synthesized cholesterol and the suppressed evolution of pyruvate-generated CO2 in tumors: further evidence for a persistent truncated Krebs cycle in hepatomas. *Biochim. Biophys. Acta*. 886:169–176.

Patterson, G. H., S. M. Knobel, P. Arkhammar, O. Thastrup, and D. W. Piston. 2000. Separation of the glucose-stimulated cytoplasmic and mitochondrial NAD(P)H responses in pancreatic islet beta cells. *Proc. Natl. Acad. Sci. USA*. 97:5203–5207.

Redmond, T. M., S. Yu, E. Lee, D. Bok, D. Hamasaki, N. Chen, P. Goletz, J. X. Ma, R. K. Crouch, and K. Pfeifer. 1998. Rpe65 is necessary for production of 11-*cis*-vitamin A in the retinal visual cycle. *Nat. Genet*. 20:344–351.

Robinson, D. W., G. M. Ratto, L. Lagnado, and P. A. McNaughton. 1993. Temperature dependence of the light response in rat rods. *J. Physiol*. 462:465–481.

Rungger-Brandle, E., H. Kolb, and G. Niemeyer. 1996. Histochemical demonstration of glycogen in neurons of the cat retina. *Invest. Ophthalmol. Vis. Sci*. 37:702–715.

Saari, J. C. 2000. Biochemistry of visual pigment regeneration: the Friedenwald lecture. *Invest. Ophthalmol. Vis. Sci*. 41:337–348.

Saari, J. C., D. L. Bredberg, and D. F. Farrell. 1993. Retinol esterification in bovine retinal pigment epithelium: reversibility of lecithin:retinol acyltransferase. *Biochem. J*. 291:697–700.

Saari, J. C., G. G. Garwin, J. P. Van Hooser, and K. Palczewski. 1998. Reduction of all-*trans*-retinal limits regeneration of visual pigment in mice. *Vision Res*. 38:1325–1333.

Shichida, Y., and H. Imai. 1999. Amino acid residues controlling the properties and functions of rod and cone visual pigments. *In* Rhodopsins and Phototransduction, Novartis Foundation Symposium 224. John Wiley & Sons, Chichester, UK. 142–153.

Tsina, E., C. Chen, Y. Koutalos, P. Ala-Laurila, M. Tsacopoulos, B. Wiggert, R. K. Crouch, and M. C. Cornwall. 2004. Physiological and microfluorometric studies of reduction and clearance of retinal in bleached rod photoreceptors. *J. Gen. Physiol*. 124:429–443.

Weng, J., N. L. Mata, S. M. Azarian, R. T. Tzekov, D. G. Birch, and G. H. Travis. 1999. Insights into the function of Rim protein in photoreceptors and etiology of Stargardt's disease from the phenotype in abcr knockout mice. *Cell*. 98:13–23.

Williams, R. M., D. W. Piston, and W. W. Webb. 1994. Two-photon molecular excitation provides intrinsic 3-dimensional resolution for laser-based microscopy and microphotochemistry. *FASEB J*. 8:804–813.

Winkler, B. S. 1981. Glycolytic and oxidative metabolism in relation to retinal function. *J. Gen. Physiol*. 77:667–692.

Winkler, B. S. 1986. Buffer dependence of retinal glycolysis and ERG potentials. *Exp. Eye Res*. 42:585–593.

Witkovsky, P., and C. Y. Yang. 1982. Uptake and localization of 3H–2 deoxy-D-glucose by retinal photoreceptors. *J. Comp. Neurol*. 204:105–116.

Zimmerman, W. F. 1974. The distribution and proportions of vitamin A compounds during the visual cycle in the rat. *Vision Res*. 14:795–802.